Optimization of dam's spillway design under climate change conditions

Ahmad Ferdowsi, Sayed-Farhad Mousavi, Saeed Farzin and Hojat Karami

ABSTRACT

The present research introduces a model to find the best shape of a dam's spillway under climate change impacts, considering a benchmark problem (i.e., Ute Dam's labyrinth spillway in the Canadian River watershed, New Mexico, USA). A spillway design is based not only on historical data but also on the future hydrologic events. Climate variables were predicted for the years 2021–2050 based on three representative concentration pathway (RCP2.6, RCP4.5, and RCP8.5) scenarios of the general circulation model from the fifth phase of the coupled model intercomparison project (CMIP5) using the statistical downscaling model. Streamflow at the USGS 07226500 streamgage was simulated by a rainfall–runoff model with predicted data. Instantaneous peak flow was estimated using an empirical method. Flood frequency analysis was used for the estimation of the design flood. The shuffled frog-leaping algorithm (SFLA) is used to optimize a labyrinth spillway design and its results were compared with two other nature-inspired algorithms: invasive weed optimization (IWO) and cuckoo search (CS). The spillway was optimized once with the actual design flood (16,143 m^3/s) and again with the design flood under climate change (12,250 m^3/s). Results revealed that optimization with realistic design flood reduced the concrete volume of the spillway by 37% and under climate change by 43% using the SFLA.

Key words | Canadian River watershed, climate change, construction cost, labyrinth spillway design, optimum design, rainfall–runoff model

Ahmad Ferdowsi
Sayed-Farhad Mousavi
Saeed Farzin (corresponding author)
Hojat Karami
Department of Water Engineering and Hydraulic Structures, Faculty of Civil Engineering,
Semnan University,
Semnan 35131-19111,
Iran
E-mail: *saeed.farzin@semnan.ac.ir*

HIGHLIGHTS

- Proposing a new framework for the evaluation of climate change impacts on dams' spillways optimum design.
- Reducing the construction cost of a dam spillway using metaheuristics.
- Comparing the performance of three nature-inspired algorithms (SFLA, IWO, and CS).
- Investigation of changes in rainfall, maximum, and minimum air temperatures in the Canadian River watershed during a 30-year period (i.e., 2021–2050).

INTRODUCTION

It is worth starting this optimization study with a very charming explanation by Yang (2010), which represented an optimization problem as treasure hunting. In this treasure hunt, treasure is hidden in a wide landscape, and like any real problem there are limitations such as time. As hunters do not know where to look for the treasure, a random walk or search is inevitable. There are some keys to perform well and find the ultimate treasure (global optimum), including a search by a group of best hunters.

Optimization may be needed in many problems in our everyday life. In today's competitive world, humans try to maximize efficiency from a limited number of available

doi: 10.2166/hydro.2020.019

resources. For this purpose, artificial intelligence or computational intelligence is used with optimization techniques (Erdik & Savci 2008; Erdik 2009; Erdik *et al.* 2009; Kaveh 2017; Bozorg-Haddad 2018; Ehteram *et al.* 2019). Normally, an optimization problem requires sophisticated optimization tools. Over the last decade, a diverse spectrum of algorithms, from traditional gradient-based algorithms and simplex methods to evolutionary algorithms and nature-inspired metaheuristics (Yang 2018), have extensively been used for dealing with highly nonlinear and tough optimization problems, in particular, problems in water engineering (Hassanvand *et al.* 2019; Monsef *et al.* 2019).

Dams, as crucial infrastructures for water supply and flood mitigation, require ancillary structures and facilities (such as spillways) to enable them to pass design floods (Novak *et al.* 2014). In terms of engineering, spillways must be able to meet the basic requirements such as hydraulic performance, structural stability, environmental impacts, and safety aspects (Ghare *et al.* 2008). A labyrinth spillway is one of the nonlinear spillways that due to its geometric shape can increase discharge capacity. The use of this spillway increases the crest length without increasing the width of the overflow span (Khatsuria 2004). The popularity of labyrinth spillways has considerably increased over the last decade, notably in the USA (Khode & Tembhurkar 2010).

While more than 100 years have passed from the introduction of labyrinth spillways (Hager *et al.* 2015), few studies have been carried out on optimum design of these structures using intelligent methods. Hosseini *et al.* (2016) proposed an optimal model for labyrinth spillways. An adaptive neural fuzzy inference system (ANFIS) model was used to calculate the discharge coefficient of the spillway and differential evolution (DE) and genetic algorithm (GA) for determining the best geometry of the labyrinth. Kardan *et al.* (2017) optimized the shape of a trapezoidal labyrinth spillway by the evaluation of the number of cycles using the GA. In the study of Tabari & Hashempour (2019), GWO-DSO (grey wolf optimization-direct search optimization) and PSO-DSO (particle swarm optimization-direct search optimization) hybrid algorithms were used to optimize labyrinth spillway dimensions. Ferdowsi *et al.* (2019) studied the effect of spillway's crest shape on optimizing of labyrinth geometry. The hybrid of bat algorithm (BA) and particle swarm optimization (PSO) algorithm was used and its results were compared with BA, PSO, and GA.

Meanwhile, the use of fossil fuels continued due to world population and industrial growth, on the one hand, and the destruction of agricultural lands and reduction of forest areas, on the other hand, have increased greenhouse gas emissions over the past decades. Climate change is a term used in scientific writings for the effects of greenhouse gases on the world climate and hydrological events. Several studies have warned about the impacts of climate change on hydrological variables, e.g. increasing evapotranspiration due to rising temperatures, fluctuating rainfall patterns, and seawater-level rise (Raju & Kumar 2018; Xing *et al.* 2018).

Climate change affects design and operation of water infrastructures such as flood control systems, hydropower plants, irrigation and drainage systems, water distribution networks, as well as water management practices (Bates *et al.* 2008). The impacts of climate change have been studied in some of the water-related items such as urban runoff (Zahmatkesh *et al.* 2015), irrigation (Ashofteh *et al.* 2014), drainage systems (Karamouz *et al.* 2013), hydropower plants (Sarzaeim *et al.* 2018), streamflow (Nazif & Karamouz 2014), water diversion systems (Karamouz *et al.* 2009), floods (Dong *et al.* 2018), evapotranspiration (Safavi *et al.* 2017), and reservoir operation (Ehteram *et al.* 2018a).

A US Army Corps of Engineers' survey on more than 80,000 dams has shown that almost 36% of the existing dams are unsafe due to various reasons, of which nearly 80% of insecurity is due to insufficient spillway capacity (Mirnaseri & Emadi 2014). Also, the international commission on large dams (ICOLD) has declared that approximately 30% of the dam failures are due to the lack of sufficient spillway capacity (Hosseini *et al.* 2016). Another major issue of the spillways is their high cost of construction. About 20% of the construction cost of small dams and 80% of large dams are allocated to the construction of spillways (Bozorg-Haddad *et al.* 2010). Therefore, on the one hand, the spillway design with sufficient capacity and also with the least cost is necessary and inevitable. On the other hand, climate change, as a prominent hydrologic uncertainty, should be considered in the design of present water resource systems.

In the current research, a novel optimization-based model is proposed in order to investigate the impact of climatic change on a dam's spillway design. This study aims

to propose a framework to reduce the construction cost of a labyrinth spillway and its design considering future climatic changes or uncertainty. A real benchmark design problem (i.e., labyrinth spillway of Ute Dam, which is built in the Canadian River watershed, New Mexico, USA, which is an impressive labyrinth spillway with 1,024.5 m length and 9.14 m height) is used as a case study. The current framework can also be used in the future designs of other water infrastructures.

CASE STUDY AND DATA COLLECTION

The case study is the labyrinth spillway of Ute Dam (Figure 1). This 36.88 m high embankment dam was built on the Canadian River, Ute Creek watershed, near Logan, New Mexico, USA, in 1962 (Houston 1982). The Ute Creek watershed is 5,335 km^2 wide. Ute Creek, a tributary to the Canadian River and the Ute Reservoir, provides most of the inflow to the Ute Reservoir. The Ute Reservoir was built for water storage for municipal, industrial, and agricultural uses. Much of the runoff from the Canadian River watershed is captured by the Conchas Reservoir, 65 km west of the Ute Dam Reservoir. Mean daily streamflow data were obtained from the USGS streamgage (USGS 07226500, Ute Creek near Logan), located immediately upstream of the Ute Reservoir and at the outlet of Ute Creek watershed (Figure 1). Daily rainfall and air temperatures of two COOP stations (Conchas Dam and Pasamonte) are used to represent weather conditions of the Ute Dam watershed (Table 1 and Figure 1).

METHODOLOGY

In the proposed approach, climatic parameters (minimum and maximum air temperatures and rainfall) are predicted in the catchment area for a period of 30 years (2021–2050). Afterwards, streamflow is simulated using the predicted data (rainfall and air temperatures). Design discharge, as a key parameter in water infrastructure designs, is calculated under climate change conditions. The shuffled frog-leaping algorithm (SFLA) is employed to determine the optimal shape of labyrinth spillway based on design discharge under climate change. The performance of SFLA is also compared with invasive weed optimization (IWO) and cuckoo search (CS) algorithms. The results are obtained by the use of the MATLAB (R2013a) software. In Figure 2, the main steps of the proposed methodology are presented.

Labyrinth spillway design

The primary hypothesis behind developing labyrinth spillways was to increase the discharge capacity through the increase of crest length in a constant width. Labyrinth spillway's cycles could have a linear configuration (e.g., trapezoidal, triangular, and rectangular) or an arced configuration (Sangsefidi *et al.* 2017; Azimi & Seyed Hakim 2019; Safarrazavi Zadeh *et al.* 2019; Ghaderi *et al.* 2020). A general form of the labyrinth spillway discharge equation is shown in the following equation:

$$Q = \frac{2}{3} C_d L \sqrt{2g} H_t^{3/2} \tag{1}$$

where Q is the discharge over the spillway, C_d is the dimensionless discharge coefficient, L is the spillway length, g is the acceleration due to gravity, H_t is the total head on the crest ($H_t = h + V^2/2g$), V is the mean cross-sectional water velocity, and h is the piezometric head upstream of the spillway relative to the spillway crest elevation. The calculation of spillway discharge depends on the exact determination of C_d value. The effects of labyrinth spillway geometry and flow conditions on discharge are represented as C_d (Crookston & Tullis 2012). To calculate the C_d, Equation (2) is used (Crookston & Tullis 2013), which was extracted from physical models of non-vented trapezoidal labyrinths with wall angles between 6° and 35° and without concerning the influence of abutments on flow. In summary, C_d is determined according to different wall angles, half-round crest shape, and headwater ratio.

$$C_d = A \times \left(\frac{H_t}{P}\right)^{B\left(\frac{H_t}{P}\right)^C} + D \tag{2}$$

where P is the crest height, and coefficients A, B, C, and D are derived from Table 2. It is worth mentioning that Equation

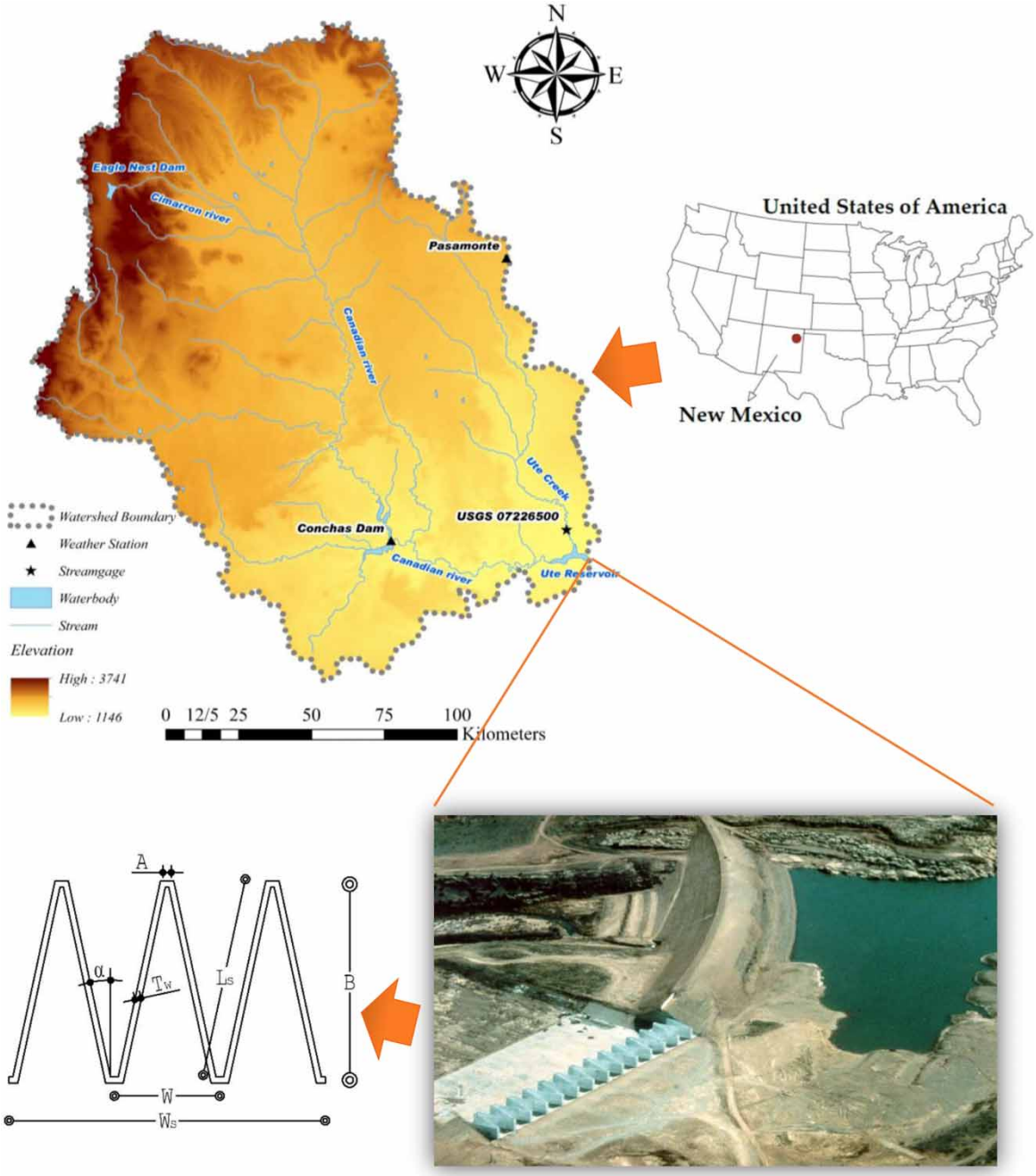

Figure 1 | Location of Ute Dam and its watershed, selected stations, dam's labyrinth spillway, and its parameters.

(2) and the coefficients in this table are derived from a figure which is provided in Crookston & Tullis (2013).

A labyrinth spillway crest profile has a noteworthy impact on discharge coefficient and thus on discharge capacity. Various forms have been proposed for the labyrinth spillway crest including flat, sharp, half-round (HR), quarter-round (QR), ogee, and WES (truncated ogee). Previous studies have proved that half-round and ogee crest profiles are more efficient crest shapes (Willmore 2004; Crookston 2010; Ferdowsi *et al.* 2019).

Table 1 | Description of the selected stations

Station	Data	Latitude	Longitude	Datum	Source
USGS 07226500, Ute Creek near Logan	Streamflow	35.44	− 103.53	1,164.3	USGS
Conchas Dam	Rain, T_{max}, T_{min}	35.41	− 104.19	1,294.4	NM Univ.
Pasamonte	Rain, T_{max}, T_{min}	36.30	− 103.74	1,723.3	NM Univ.

Note: T_{max} and T_{min}, maximum and minimum air temperatures; USGS, US Geological Survey; NM Univ., Website of Climate Center, New Mexico University.

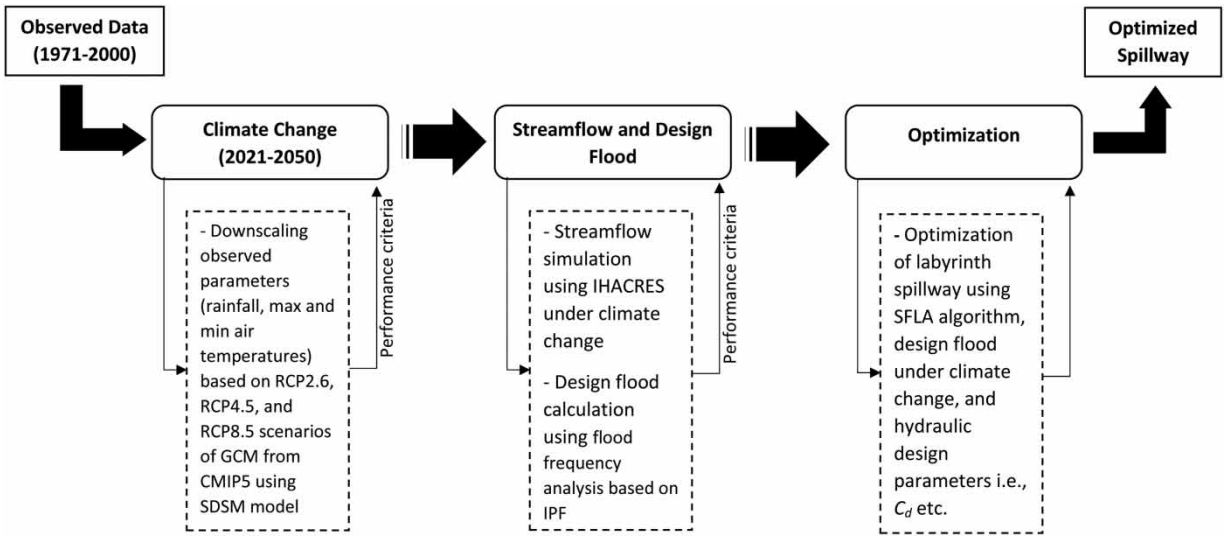

Figure 2 | Flowchart of the proposed methodology.

Table 2 | Curve-fit coefficients for half-round labyrinth spillway, validated for $0.05 \leq H_t/P < 0.9$ (Crookston & Tullis 2013)

α	A	B	C	D
6°	0.009447	−4.039	0.3955	0.1870
8°	0.017090	−3.497	0.4048	0.2286
10°	0.029900	−2.978	0.4107	0.2520
12°	0.030390	−3.102	0.4393	0.2912
15°	0.031600	−3.270	0.4849	0.3349
20°	0.033610	−3.500	0.5536	0.3923
35°	0.018550	−4.904	0.6697	0.5062

The geometry of each structure determines the volume of materials needed for its construction and also its construction costs and time. Therefore, by optimizing the geometry of a spillway, the lowest volume of concrete and cost may be achieved. The total concrete volume of a trapezoidal labyrinth spillway (V_T) consists of three parts (Figure 3): V_W (volume of spillway wall), V_e (volume of the end walls), and V_S (volume of floor slab) (Falvey 2003) as follows:

$$V_W = N \times L_c \times P \times T_w \quad (3)$$

$$V_e = 2 \times (P + H_t + F_b) \times (B + H_t) \times T_w \quad (4)$$

$$V_S = (B + 2H_t) \times W_w \times T_s \quad (5)$$

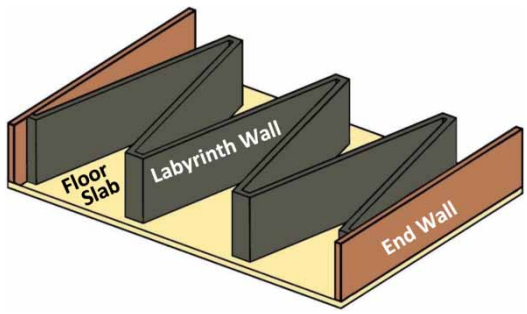

Figure 3 | Illustration of different parts of a labyrinth spillway.

where N is the number of cycles, P is the crest height, T_w is the wall thickness, F_b is the freeboard, H is the total head, and B is the labyrinth length (parallel to flow).

Labyrinth spillway optimum design

To solve an optimization problem, it is needed to determine some terms and functions, including objective function, constant parameters, design variables, and constraints (penalty functions). The objective function in the optimization of labyrinth spillway geometry includes three parts: volumes of labyrinth wall, end walls, and floor slab (Equations (3)–(5) and Figure 3). Hence, the objective function can be formulated as follows:

$$\text{Minimize } f_{\text{Cost}} = V_T = V_W + V_e + V_s \tag{6}$$

In optimization, some parameters are considered constant based on engineering judgment and previous studies. These parameters, in addition to reduce the dimensions of the problem, will also have a significant effect on saving a computational time. These parameters in the present study are free board ($F_b = 0.6$ m), slab thickness ($T_s = 0.3$ m), number of cycles ($N = 14$), and crest shape (HR).

On the other hand, design variables are considered unknown and their values are calculated in the optimization process. Design variables in this study are crest height (P), total head (H_t), labyrinth length parallel to flow (B), wall thickness (T_w), angle of side legs (α), and apex center-line width (A).

The values of the design variables must be within a certain range. In other words, optimizing the value of the objective function is not possible at any cost. These limitations (or constraints), which are the results of previously constructed spillways, laboratory tests, numerical modeling, and codes (Chen 2015), improve labyrinth performance and its safety. The penalty method is a common method to handle constraints into objective functions, which is used in the present study. The following section discusses the penalty functions.

According to the first penalty (i.e., Equation (7)), the discharge of optimal labyrinth spillways will be equal to the flood design (Q_d) of Ute labyrinth:

$$f_{p1} = (Q_d - 2/3\sqrt{2g}C_d L H_t^{3/2}) \le 0 \tag{7}$$

The labyrinth spillway loses its efficiency by increasing its head. A headwater ratio is defined as the total head (H_t) divided by the height of spillway crest (P). Generally, labyrinth spillways are designed for a headwater ratio of less than 0.9 (Crookston 2010). Crookston & Tullis (2013) used the headwater ratio of 0.05–0.9. The following penalty function is expressed to design an optimum labyrinth with a headwater ratio between 0.05 and 0.9:

$$f_{p2} = \left(1 - \frac{H_t}{0.05P}, \frac{H_t}{0.9P} - 1\right) \le 0 \tag{8}$$

A relative thickness ratio is calculated by dividing the height of spillway crest (P) by spillway wall thickness (T_w). Wall thickness depends on the hydraulic forces, ice loading, and site conditions and is calculated from structural analysis. Tullis *et al.* (1995) mentioned that a major decrease in wall thickness causes separation and reduces the discharge coefficient. Their models are based on $T_w = P/6$. Some studies have used models which are based on $T_w = P/8$ (Willmore 2004; Crookston & Tullis 2013). Equation (9) is written as a penalty function to control wall thickness and the spillway crest height of optimum models:

$$f_{p3} = \left(1 - \frac{P}{6T_w}, \frac{P}{8T_w} - 1\right) \le 0 \tag{9}$$

A magnification ratio is the length of a spillway cycle (L_c) to the cycle width (W). Previous optimization studies have recommended that this ratio must be limited to a range of 3–9.5 for optimal performance (Kardan *et al.* 2017). The penalty function of this ratio is considered as follows:

$$f_{p4} = \left(1 - \frac{L_C}{3W}, \frac{L_C}{9.5W} - 1\right) \le 0 \tag{10}$$

One cycle width (W) divided by crest height (P) is described as the cycle width ratio (or vertical aspect). Crookston & Tullis (2013) suggested that this ratio should be limited to 2–4. The following equation is used as the penalty function of cycle width ratio:

$$f_{p5} = \left(1 - \frac{W}{2P}, \frac{W}{4P} - 1\right) \le 0 \tag{11}$$

The apex width (A) divided by the cycle width (W) is described as the apex ratio. This ratio should be as low as possible, usually, equal to 0.0765 or less (Hepler 1992). The penalty function is written as follows:

$$f_{p6} = \left(\frac{A}{0.0765W} - 1\right) \leq 0 \tag{12}$$

A wall thickness ratio is obtained by dividing the apex width (A) by the spillway wall thickness (T_w). Tullis *et al.* (1995) limited this ratio to 1–2 for optimum performance. Here, its penalty function is considered as follows:

$$f_{p7} = \left(1 - \frac{A}{T_w}, \frac{A}{2T_w} - 1\right) \leq 0 \tag{13}$$

The ratio of interference length (L_D) to one side-leg length (L_S) is important for limiting the effects of nappe interference, which reduces spillway discharge efficiency. Indelkofer & Rouve (1975) explored the idea of nappe interference and introduced a nappe effective disturbance length. Falvey (2003), by using data from previous studies and labyrinth spillway models, proposed this ratio as Equation (14) and notified that this ratio should be equal to 0.30 or less. However, data presented by Falvey (2003) indicated a limit of 0.35 (Crookston & Tullis 2012). Therefore, its penalty function can be considered as Equation (15):

$$\frac{L_D}{L_S} = 0.244 \ln\left(\frac{H_t}{P}\right) + (0.94 - 0.03\alpha) \tag{14}$$

$$f_{p8} = \left(\frac{L_D}{0.35L_S} - 1\right) \leq 0 \tag{15}$$

Optimization tool: shuffled frog-leaping algorithm

The SFLA has been introduced by Eusuff & Lansey (2003). It was originally used to optimize the design of water distribution networks and is based on random and deterministic procedures. This algorithm employs a memetic metaheuristic approach based on the natural behavior of frogs. High performance, simple concept, few parameters, and easy programming are some key advantages of SFLA (Li *et al.* 2010). Initially, the SFLA generates an initial random population of P frogs (i.e., solutions). The location of the ith solution (frog) is represented as $X_i = (X_{i1}, X_{i2}, \ldots, X_{iD})$, where D is the variable number. Afterwards, sorting of the frogs is performed in a descending order based on their fitness. In the next step, all members of the population are divided into m subsets referred to as memeplexes, each containing frogs (i.e., $P = m \times n$). The frog with the best performance (according to the objective function) is placed in the first memeplex, the second best frog is placed in the second memeplex, and the mth frog is placed in the mth memeplex. In the next division process, the $(m+1)$th frog is placed in the first memeplex. The positions of the best and worst frogs, in each memeplex, are identified as X_b and X_w, respectively. In addition, X_g is identified as the position of a frog with the global optimum. A similar process which exists in the PSO algorithm is applied to enhance the frog with the worst fitness in each cycle, within each memeplex. As a result, the position of the frog, which has the worst fitness, goes toward the position of the frog, which has the best fitness, as follows:

$$D_i = \text{rand} \times (X_b - X_w) \tag{16}$$

$$X_w^{new} = X_w^{old} + D_i (D_{i\_min} < D_i < D_{i\_max}) \tag{17}$$

where D_i is the change of the frog position, rand is the random number between 0 and 1, $X_w^{new}$and X_w^{old} are new and old (i.e., current) positions, and D_{i_min} and D_{i_max} are minimum and maximum step sizes for the position of a frog, respectively.

The SFLA has shown superior performance over improved ant colony optimization, ant colony optimization, simulated annealing, Lagrange multiplier method, PSO, and GA in the previous studies (Orouji *et al.* 2012, 2016).

Climate change

Scientific research has shown that climate change has considerable impacts on rainfall, temperature, evapotranspiration, streamflow, and water resources. To simulate the effects of future climate conditions, the output from global coupled atmospheric-ocean general circulation models (coupled GCMs) is used as the input to hydrologic. In the present study, a low greenhouse gas emission scenario (RCP2.6), a medium emission scenario (RCP4.5), and a

very high emission scenario (RCP8.5) are used. These scenarios are introduced in the fifth phase of the coupled model intercomparison project (CMIP5) of the GCM. In recent years, there has been considerable focus on the use of these new RCP scenarios.

Statistical downscaling model

Statistical downscaling model (SDSM), developed by Wilby *et al.* (2002), is a combination of regression and conditional weather generator technique. SDSM relies on empirical relationships between local scale predictand(s) and regional scale predictor(s). The model performance has been acceptable in different studies (Sarzaeim *et al.* 2017; Xing *et al.* 2018). Key functions are quality control and data transformation, selection of downscaling predictor variables, model calibration, weather generator, data analysis, graphical analysis, and scenario generation.

Rainfall–runoff model

In the present study, a hydrologic model based on unit hydrograph theory (i.e., IHACRES) is used for streamflow simulation based on observed data (1971–2000) and predicted for the near-future period (2021–2050). Hydrologic models are essential tools for assessing runoff changes in the catchment area of interest in the evaluation of the impacts of climate change (Najafi *et al.* 2011). The IHACRES is a lumped and hybrid conceptual-metric model that can simulate streamflow with minimum input data, i.e., rainfall and temperature (or potential evapotranspiration) at two steps: (1) a nonlinear loss module and (2) a linear unit hydrograph module. At the first step, rainfall is converted to effective rainfall and then runoff is produced in the second step (Jakeman *et al.* 1990; Croke *et al.* 2005). Despite the simplicity of IHACRES structure, the model has performed well in many catchments worldwide (Sarzaeim *et al.* 2017; Ehteram *et al.* 2018b).

Design flood

Engineers, hydrologists, and agriculturalists often need the design flood for the design of hydraulic structures, such as dams, spillways, bridges, channels, or culverts. Design flood estimation is a prerequisite for planning, design, and management of hydraulic structures and has a crucial impact on the investment and benefits of the projects, and also on their safety (Duricic *et al.* 2013; Erdik *et al.* 2013; Pektas & Erdik 2014; Bhagat 2017; Guo *et al.* 2018).

Flood frequency analysis

Generally, design flood is estimated from flood frequency analysis when sufficiently long observed streamflow records are available. The main modeling problem in flood frequency analysis is the selection of a probability distribution for flood magnitudes (Guo *et al.* 2018). Gumbel, generalized extreme value, log-normal, and log-Pearson type III distributions are widely used in analyzing annual maximum series (Wilks 1993). The general equation of frequency analysis is given as follows:

$$Q_{T_r} = \overline{Q} + K \times s \tag{18}$$

where Q_{T_r} is design flood with a return period of T_r, K is a frequency factor, and $\bar{Q}$ and s are average and standard deviation of maximum instantaneous flows, respectively.

Instantaneous peak flow

Generally, the design of hydraulic structures for flood control is conducted with instantaneous peak flow, i.e. IPF (Fill & Steiner 2003). However, the data relating to mean daily flow (MDF) are the most common recorded hydrological variable. The design of control structures using MDF data may cause underestimation, with a consequent risk of possible failure (Taguas *et al.* 2008). The following methods are used to estimate IPF from MDF.

Fuller (1914) studied flood data of some watersheds in the USA and suggested the following equation:

$$\mathrm{IPF} = \mathrm{MDF} \times (1 + 2.66 \times A^{-0.3}) \tag{19}$$

Sangal (1983), based on a triangular hydrograph, proposed Equation (20), which is tested by some streamgauge

data in Ontario, Canada:

$$\mathrm{IPF} = \frac{4 \times \mathrm{MDF} - Q_1 - Q_2}{2} \tag{20}$$

Fill & Steiner (2003) used data from watersheds in Brazil and proposed the following equation:

$$\mathrm{IPF} = \frac{0.80 \times \mathrm{MDF} + 0.25 \times (Q_1 + Q_2)}{0.9123 \times (Q_1 + Q_2)/2 \times Q_2 + 0.36} \tag{21}$$

where IPF is in m^3/s, MDF is in m^3/s, A is the drainage area (km^2), Q_1 is the mean daily flow in the preceding day (m^3/s), and Q_2 is the mean daily flow in the following day (m^3/s).

Performance assessment criteria

Various indices may be used to show the performance of simulation models. In the current study, the performance of SDSM and IHACRES models was assessed with three statistics, namely correlation coefficient (R), Nash–Sutcliffe efficiency (NSE), and relative bias (Bias) listed in Table 3 (Xing *et al.* 2018). The accepted values for streamflow predictions suggested by Moriasi *et al.* (2007) are $0.5 < \mathrm{NSE} \leq 1$ and $-25\% \leq \mathrm{Bias} \leq +25\%$.

RESULTS AND DISCUSSION

SDSM calibration and validation

In the SDSM, calibration is done by the model itself, which only needs the length of the period to be determined. The length of the calibration and validation periods can vary considering the total length of the base period. In the present study, the total length of the base (observation) period was selected from January 1971 to December 2000 (30 years). The calibration period was 1971–1991 (70% of the data), and 30% of the data (1992–2000) was chosen for the validation phase. Results of the validation period are presented in Table 4 using statistical indices (R, NSE, and Bias) for both stations. These results are calculated based on the SDSM output for rainfall variables, maximum and minimum air temperatures over the 9 years (1992–2000) compared with the observed values. According to the statistical indicators of Table 4, the SDSM has a good performance in the studied area.

A closer examination of the results of the correlation indices shows that, in general, the SDSM is more capable of modeling temperature than rainfall. In other words, based on Table 4, R and NSE indices for air temperatures were greater than for rainfalls. Also, Bias values for temperatures are less than for rainfall, except for minimum temperature in the Conchas Dam station. A graphical representation of the results of simulation of average monthly rainfall, and maximum and minimum temperatures in the validation period for the two stations are shown in Figure 4.

Table 4 | Performance assessment of monthly observed and simulated results (SDSM output) during the validation period (1992–2000)

		Statistical criteria		
Station	**Variables**	***R***	**NSE**	**Bias (%)**
Conchas Dam	Rain	0.930	0.807	−4.991
	T_{max}	0.996	0.975	4.134
	T_{min}	0.998	0.990	5.735
Pasamonte	Rain	0.926	0.838	8.598
	T_{max}	0.998	0.992	1.398
	T_{min}	0.999	0.991	6.982

Table 3 | Equations of performance assessment criteria

Index	Equation
Correlation coefficient	$R = \sum_{i=1}^{n} (O_i - \bar{O}) \times (S_i - \bar{S}) / \left[\sum_{i=1}^{n} (O_i - \bar{O})^2 \times (S_i - \bar{S})^2\right]^{0.5}$
Nash–Sutcliffe efficiency	$\mathrm{NSE} = 1 - \sum_{i=1}^{n} (O_i - S_i)^2 / \sum_{i=1}^{n} (O_i - \bar{O})^2$
Relative bias	$\mathrm{Bias} = \sum_{i=1}^{n} (O_i - S_i) / \sum_{i=1}^{n} (O_i) \times 100$

Note: O_i is the observed value, $\bar{O}$ is the average of observed values, S_i is the simulated value, $\bar{S}$ is the average of simulated values, and n is the number of time-steps.

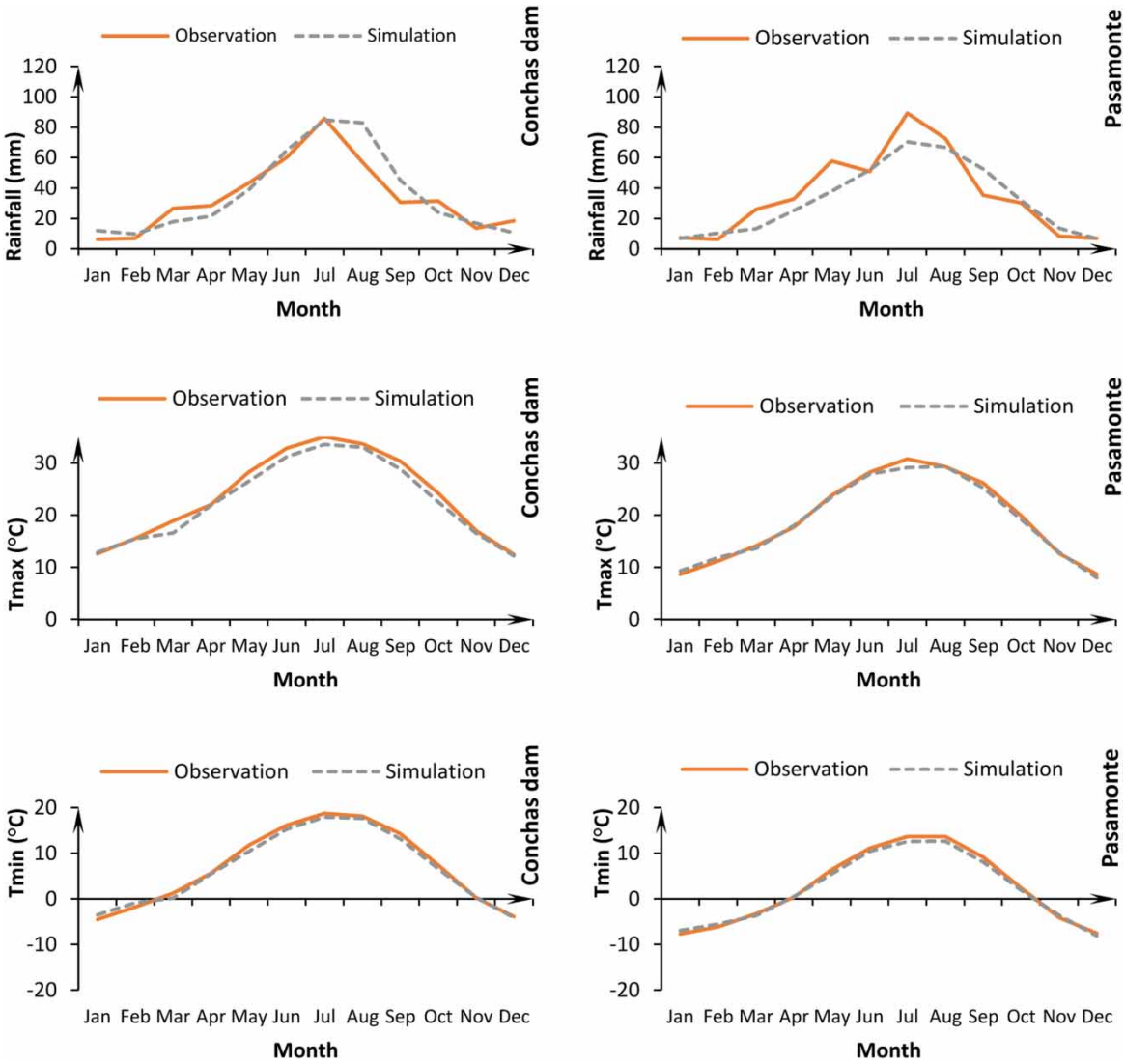

Figure 4 | Comparison of average monthly rainfall, maximum air temperature (T_{max}), and minimum air temperature (T_{min}) in the validation period (January 1992–December 2000) simulated by the SDSM.

Rainfall under climate change

At first, the performance of the SDSM was assured. Afterwards, using the SDSM and the downloaded datasets, the daily rainfall, maximum temperature, and minimum temperature for the near-future period (2021–2050) were downscaled. Rainfall, maximum temperature, and minimum temperature increased at both stations under all three RCPs (Figure 5). For instance, the observed mean annual rainfall at the Pasamonte station increased from 415.4 mm in the base period to 477.3 mm in the near-future period based on RCP4.5. The forecast for rainfall at the Conchas Dam was similar. In a study by Brauer *et al.* (2015), flow and rainfall trends were compared during the baseline (1971–2000) and the 2001–2010 period in the Canadian River watershed in the Upper Lake Meredith in New Mexico and Texas. Among the stations in this study, rainfall at six stations had an increasing trend in the 10-year observation period compared with the base period. Among these six stations, there are three stations (Eagle Nest, Ocata, and Villanueva) in New Mexico and near the studied stations in the present study. The Villanueva station had the highest rainfall. The mean annual

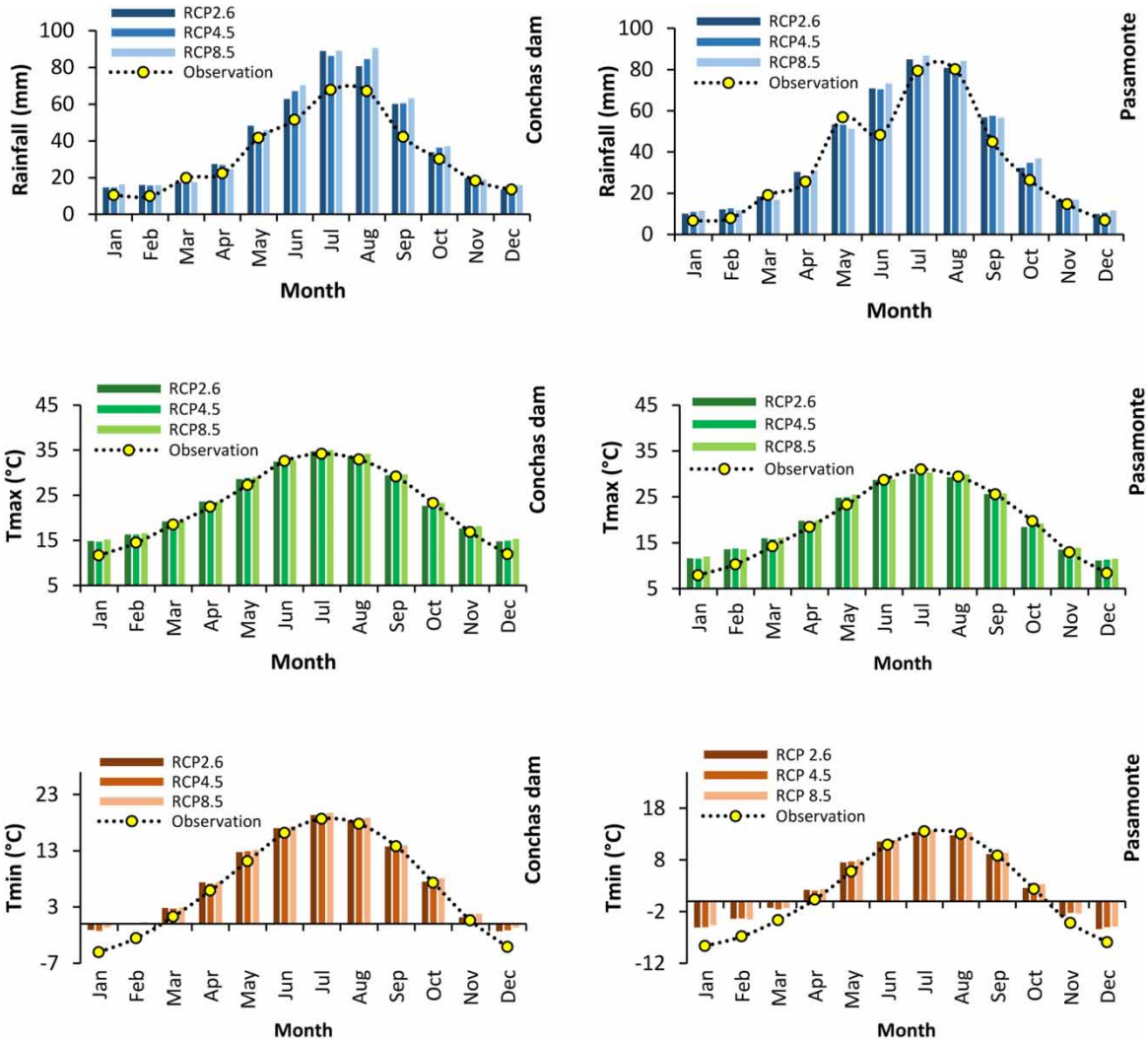

Figure 5 | Comparison of mean monthly rainfall, maximum air temperature (T_{max}), and minimum air temperature (T_{min}) under RCP2.6, RCP4.5 and RCP8.5 scenarios, in 1971–2000 and 2021–2050.

rainfall of the Villanueva station during the observation period was 231 mm, which, with 216 mm increment in the 2001–2010 period, rose to 447 mm. It can be seen that in the watershed, the increase in rainfall has also occurred according to the past research based on observed data.

Air temperature under climate change

The maximum temperature will increase at both stations based on RCP scenarios. The maximum temperature of the Conchas Dam station was 22.92 °C in the observation period, reaching 24.22, 24.31, and 24.57 °C, respectively, in the RCP2.6, RCP4.5, and RCP8.5 scenarios. At the Pasamonte station, there is also a similar trend. The maximum observed temperature at this station was 19.14 °C, which will increase in the future period and, according to the three scenarios, will reach 20.40, 20.50, and 20.75 °C. The minimum temperature, like the maximum temperature, shows an increasing trend at both stations. The minimum temperature at the Conchas Dam was 6.75 °C during the observation period, and by the influence of climate change, it will reach 8.25, 8.36, and 8.62 °C in the RCP2.6, RCP4.5, and RCP8.5 scenarios. At the Pasamonte station, the minimum observed temperature was 1.95 °C, which in

Table 5 | Performance assessment of the IHACRES model in the calibration and validation periods in both stations

Station	Period	Length (day)	Index		
			R	NSE	Bias (%)
Conchas Dam	Calibration	3,580–4,825	0.8	0.7	− 21.0
	Validation	7,903–8,225	0.8	0.6	− 7.5
Pasamonte	Calibration	3,580–4,825	0.9	0.7	− 18.7
	Validation	7,565–7,609	0.9	0.9	4.4

the near future will be 3.44, 3.57, and 3.78 °C, according to the three RCP scenarios.

IHACRES calibration and validation

Table 5 shows the results of calibration and validation of the observed daily flow data of the two stations of USGS 07226500. Based on the three performance criteria, both stations have an acceptable status in both calibration and validation periods. In other words, the value of *R* is close to 1, NSE is more than 0.7, and the Bias index is in the ±25% range.

Streamflow simulation

After assuring the performance of the IHACRES model in simulation of observed streamflow, it can be used to simulate streamflow using downscaled data from the SDSM for the 2021–2050 period. For this purpose, rainfall and temperature data of the two stations were imported into IHACRES with daily time-steps. In Figure 6, the mean annual streamflow for the base period for the USGS 07226500 station with the simulated streamflow of the upcoming period, using the RCP2.6 for each of the two stations, is shown. According to Figure 6, the mean observed streamflow is less than the flow in the future period in both stations. In the present study, the peak flow is used to calculate design flood. Figure 7 shows the peak streamflow of 30 years in both past and future periods. In this figure, in contrast to Figure 6, the observed streamflow values are higher than the simulated ones. With rainfall and temperature increasing in the studied watershed, the amount of streamflow increased, and peak streamflow values decreased. This is due to the proximity of predicted rainfall values to normal values and the reduction of their standard deviations relative to the observation period. The predicted rainfall, instead of concentrating in a few days, will occur in a larger time period, which, in turn, produces peak daily discharge. This can be an outcome of using the SDSM downscaling model.

DESIGN FLOOD

Instantaneous peak flow

The performance of three empirical equations (Fuller, Sangal, and Fill-Steiner) in IPF estimation was investigated. According to the performance criteria, the Fuller's equation was recognized as the best method ($R = 0.9$, NSE = 0.9, and Bias = 16.9) for converting MDF to IPF.

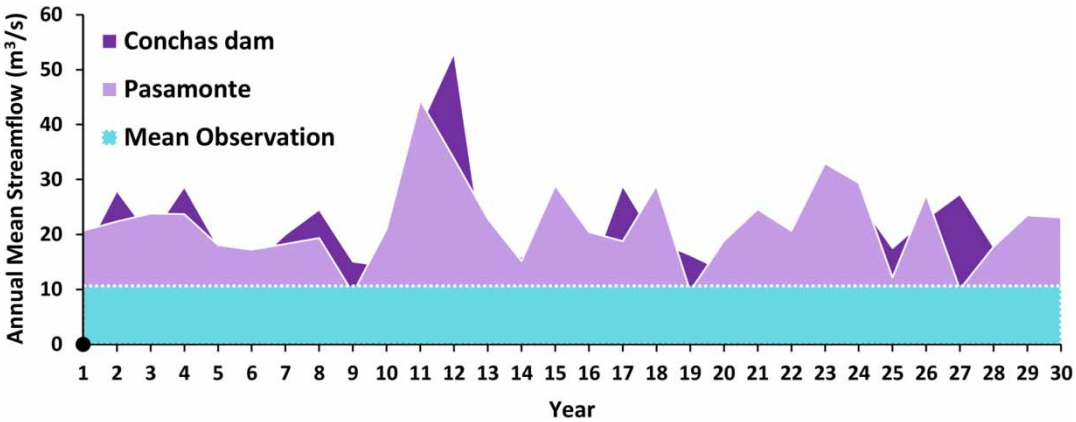

Figure 6 | Comparison of observed mean annual streamflow (based on mean daily flows in 1971–2000) and simulated mean annual streamflow (in 2021–2050) in Conchas Dam and Pasamonte stations using the RCP2.6 scenario.

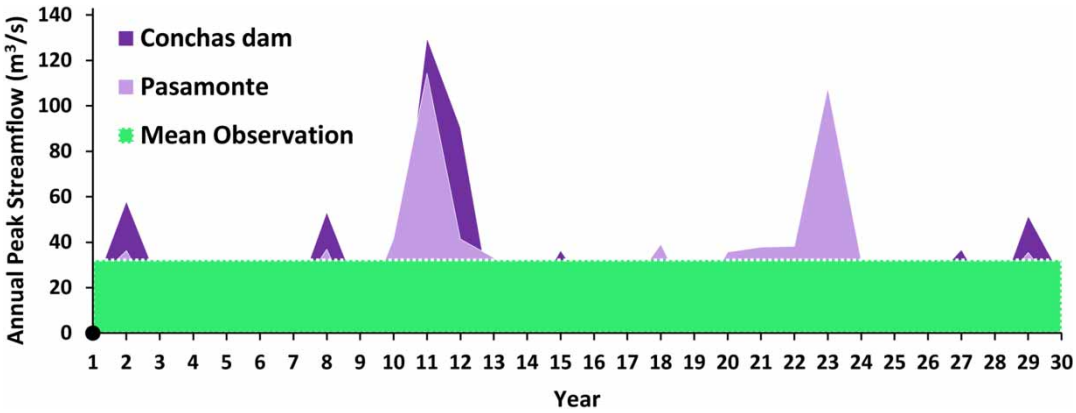

Figure 7 | Comparison of observed mean annual peak streamflow (based on mean daily in 1971–2000) and simulated mean annual peak streamflow (2021–2050) in Conchas Dam and Pasamonte stations using the RCP2.6 scenario.

Flood frequency analysis

To determine the design flood of the labyrinth spillway using the flood frequency analysis method, an appropriate distribution was selected first based on the maximum annual peak streamflow in the base period. Subsequently, using this distribution and the amount of actual design flood of Ute spillway (16,143 m^3/s), the return period of the Ute spillway was determined (as described by Equation (8)). The calculated return period was used to determine the simulated design flood for the future period with the IHACRES model. Since in this study, only the annual peak streamflow (with constant return period) was required to determine the design flood of the future period, using three-parameter distributions such as Pearson type III and log Pearson type III, was practically impossible to determine the coefficient K in Equation (18). Therefore, among the two-parameter distributions, the Gumbel distribution was selected after a Kolmogorov–Smirnov (K–S) fitting test. According to Table 6, the observed and predicted data fitted to the four statistical distributions such as extreme value distribution, log Pearson type III, Gumbel, and log-normal. The normal distribution is the only distribution that does not fit the three IPF series.

There were other reasons for choosing Gumbel distribution. Commonly, Gumbel distribution is used for predicting extreme events (i.e., floods) in hydrology (Haan 1977; Cunnane 1989). Onen & Bagatur (2017) chose Gumbel distribution for several reasons such as: (1) the relatively long streamflow data (>10 years) and (2) the river is less regulated; hence is not significantly affected by reservoir operations, diversions or urbanization, which is true in the present study. The return period of the design flood of the Ute spillway (16,143 m^3/s) would be 100,000 years by the Gumbel distribution. Calculation of design flood for future period was also based on the same calculated return period so that by equating all the conditions, the effect of climate change phenomenon (i.e., reduction of peak discharge) on the design flood is taken into

Table 6 | Results of the Kolmogorov–Smirnov test for each probability distribution

	Base period (USGS 07226500) Significance level (α)				Predicted period (Conchas Dam) Significance level (α)				Predicted period (Pasamonte) Significance level (α)			
Distribution	**0.1**	**0.05**	**0.02**	**0.01**	**0.1**	**0.05**	**0.02**	**0.01**	**0.1**	**0.05**	**0.02**	**0.01**
Generalized extreme value	✓	✓	✓	✓	✓	✓	✓	✓	✓	✓	✓	✓
Log-Pearson type III	✓	✓	✓	✓	✓	✓	✓	✓	✓	✓	✓	✓
Gumbel	✓	✓	✓	✓	✓	✓	✓	✓	✓	✓	✓	✓
Normal	×	✓	✓	✓	×	×	✓	✓	×	×	✓	✓
Log-normal	✓	✓	✓	✓	✓	✓	✓	✓	✓	✓	✓	✓

account. According to Table 7, the observed IPF was 170 m^3/s, which has been changed by simulation in both Conchas Dam and Pasamonte stations. According to this table, at both stations, and under climate change conditions, the maximum and minimum predicted streamflow are less than the observed values, reducing the design flood from 16,000 to 12,250 m^3/s (average of the two stations).

Canadian River watershed: past (1941–2016) and future (2021–2050)

Figure 8 is based on the peak observed streamflow of the USGS 07226500 station during the 1941–2016 period. This information was extracted from the USGS website. A linear trendline of these data is also plotted in Figure 8. The observed data from 1941 to 2016 in this figure confirms the reduction of peak streamflow (present research findings) at this station. Several studies (e.g., Wilson & O'Brien 2000; King *et al.* 2006; Spencer & Salazar 2010) have been conducted on the causes of reduced water storage in dams on the Canadian River. Different assumptions have been made according to these studies, such as: (1) changes in baseflow due to reductions in seepage from the neighboring Ogallala aquifer, (2) brush invasion, and (3) changes in rainfall patterns. According to Spencer & Salazar (2010), there is no significant change in annual rainfall in the watershed between Ute and Meredith reservoir. These results are different from those of Brauer *et al.* (2015). According to the results of this study, the main cause of the flood-pattern disruption in the Canadian River watershed is the change in the rainfall pattern (in other words, the lesser frequency of huge rainfall events). According to Brauer *et al.* (2015), the peak rainfall (i.e., occurrence of 50.9–139.7 mm rainfalls) in the 1960–1979 and 1990–2009 periods was 0.9% and in 2000–2009 was 0.3% of total rainfall, which means a decrease in peak. This is almost the same as the results of the present study.

Optimization

Labyrinth spillway optimization was performed considering the following six models: SFLA-Base, IWO-Base, and CS-Base models used SFLA, IWO, and CS algorithms, respectively, which are based on the actual design flood of Ute spillway (16,143 m^3/s) and SFLA-RCP2.6, IWO-RCP2.6, and CS-RCP2.6 models are based on design flood under climate change (12,250 m^3/s).

Sensitivity analysis of the algorithms

A sensitivity analysis on the SFLA parameters was performed to obtain the best performance. The number of frogs, memeplexes, and the maximum number of iterations were determined as 50, 5, and 1,000, respectively. In order to implement the IWO sensitivity analysis, the initial population of 10, 20, and 30; the maximum number of population of 50, 75, 100, 150, and 200; the minimum number of seeds of 0, 1, and 2; the maximum number of seeds of 2, 5, and 10; and the nonlinear modulation index of 2, 3, and 5 were considered. In CS sensitivity analysis, P_a parameter of 0.15, 0.20, and 0.25; best number of host birds' nests (or population size) of 15, 20, and 25; and different numbers of iterations were assumed. The best values for these parameters are shown in Table 8. According to this table, the best value for parameter P_a is 0.15. For the number of host nests, the minimum value of the objective function is 20 nests. Also, the CS algorithm converged after 1,000 runs, and the objective function did not change by increasing the number of iterations. The values of minimum, average, maximum, and coefficient of variation for the 10 runs are listed in Table 9. According to this table, the best values of objective function were 9,351.170 and 8,440.865 m^3 for the SFLA-Base and SFLA-RCP2.6, respectively. The models based on the SFLA, IWO, and CS

Table 7 | Description of design flood based on observed and predicted data using the Gumbel distribution

Design flood (m^3/s)	Minimum (m^3/s)	Maximum (m^3/s)	Year	Feature	Station
16,143	0.54	170.28	1971–2000	Observation	USGS 07226500
12,493	8.17	156.16	2021–2050	RCP2.6	Conchas Dam
12,007	5.09	137.53	2021–2050	RCP2.6	Pasamonte

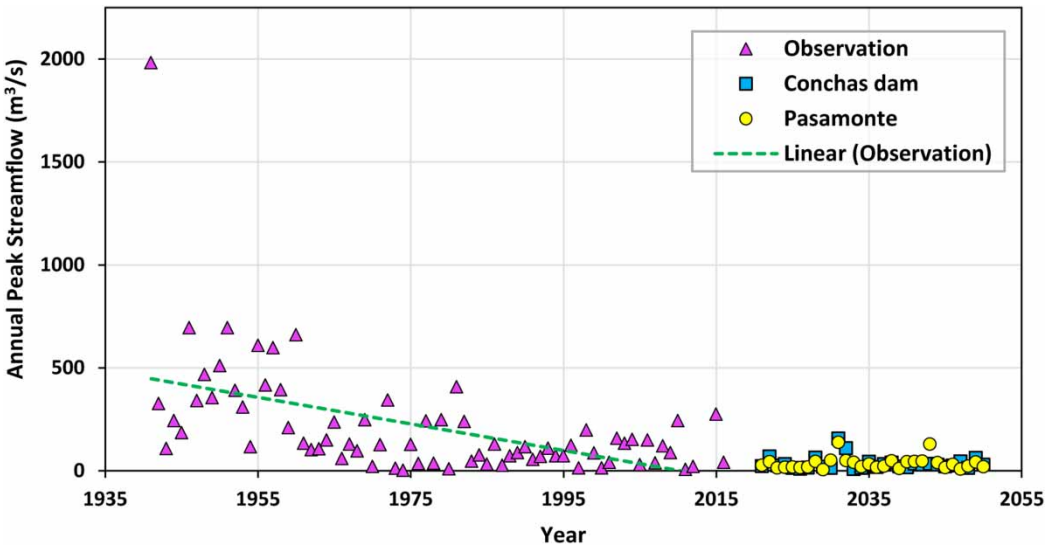

Figure 8 | Annual observed peak streamflow at USGS 07226500 Ute Creek near Logan, New Mexico, for the observed period (1941–2016) and the simulated period (2021–2050).

Table 8 | Values of parameters for labyrinth spillway optimization by SFLA, IWO, and CS

	Parameter	Symbol	Value
SFLA	Number of frogs	N	50
	Number of memeplexes	M	5
	Maximum number of iterations	it_{max}	1,000
IWO	Number of initial population	N_0	20
	Maximum number of population	p_{max}	150
	Minimum number of seeds	S_{min}	2
	Maximum number of seeds	S_{max}	5
	Nonlinear modulation index	n	3
	Initial value of standard deviation	$\sigma_{initial}$	1
	Final value of standard deviation	σ_{final}	0.001
	Maximum number of iterations	it_{max}	1,000
CS	Detection probability of the eggs	p_a	0.15
	Host nests (population size)	n	20
	Maximum number of iterations	it_{max}	1,000

convergence graphs are shown in Figure 9 for 1,000 iterations.

Optimal labyrinth spillways

The properties of Ute labyrinth spillway and proposed optimized labyrinth spillways, based on actual design flood (base model) and under climate change conditions (RCP2.6 model) using SFLA, IWO, and CS algorithms, are shown in Table 10. The spillway discharge, calculated according to Equation (1), depends on discharge coefficient (C_d), total length of the spillway (L), and total upstream head (H_t). All six models have the same discharge capacity of their design flood (16,143 and 12,250 m^3/s) or more. The total length of SFLA-Base, IWO-Base, and CS-Base models decreased by 30%, i.e., from 1,024.529 m (Ute labyrinth) to 720.469, 719.321, and 722.089, respectively. The SFLA-RCP2.6, IWO-RCP2.6, and CS-RCP2.6 models' total length also decreased by 35% to 671.334, 671.383, and 684.991 m, respectively. According to Table 10, all six models have a smaller concrete volume than the Ute spillway volume (14,789.391 m^3). The total concrete volume of SFLA-Base, IWO-Base, and CS-Base spillway models was calculated as 9,342.012, 9,368.336, and 1,0038.766 m^3, respectively (36.83, 36.66, and 32.12% lower than the Ute labyrinth spillway). The SFLA-RCP2.6, IWO-RCP2.6, and CS-RCP2.6 have minor discharge design and hence smaller concrete volume (42.96, 42.89, and 40.53% lower than the Ute labyrinth spillway, respectively). According to Table 10, the labyrinth spillway using SFLA has less concrete volume than the optimal spillways using IWO and CS algorithms. The volume of spillway walls has the greatest effect on the total concrete volume of labyrinth spillway. This volume has been reduced from 9,972.916 to 5321.531 m^3

Table 9 | Results of 10 runs of SFLA, IWO, and CS

	Objective function (m^3)					
	SFLA		IWO		CS	
Run no.	Base	RCP2.6	Base	RCP2.6	Base	RCP2.6
1	9,351.638	8,438.257	9,369.668	8,446.162	10,040.286	8,795.063
2	9,343.536	8,440.865	9,374.560	8,446.911	10,038.857	8,794.675
3	9,349.027	8,436.49	9,376.578	8,445.586	10,042.973	8,794.974
4	9,347.029	8,440.031	9,370.338	8,446.927	10,039.304	8,795.805
5	9,348.046	8,439.222	9,371.694	8,447.760	10,039.180	8,794.649
6	9,342.012	8,436.664	9,376.718	8,447.280	10,038.766	8,794.888
7	9,346.753	8,437.791	9,373.106	8,448.333	10,038.918	8,794.881
8	9,345.483	8,439.898	9,368.606	8,448.155	10,042.396	8,795.249
9	9,351.170	8,436.333	9,372.481	8,446.112	10,039.045	8,795.100
10	9,344.193	8,436.724	9,368.336	8,456.228	10,039.830	8,794.989
Minimum	9,342.012	8,436.333	9,368.336	8,445.586	10,038.766	8,794.649
Average	9,346.889	8,438.227	9,372.209	8,447.945	10,039.956	8,795.027
Maximum	9,351.170	8,440.865	9,376.718	8,456.228	10,042.973	8,795.805
Coefficient of variation	0.00034	0.00020	0.00033	0.00036	0.00015	0.00004

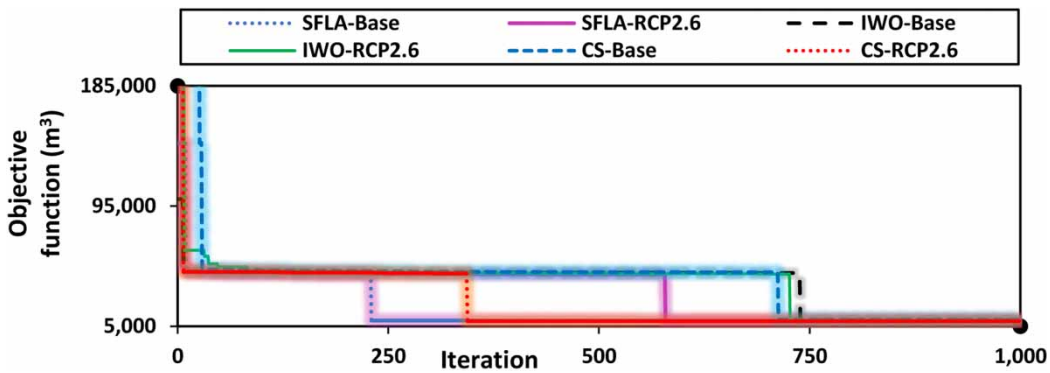

Figure 9 | Convergence of SFLA, IWO, and CS.

in the SFLA-RCP2.6 model, which means almost 50% lower than the built Ute spillway walls. The volume of end walls has been reduced by more than 37% and the volume of spillway floor slab has decreased by about 35%. Spillway crest height (P) has decreased in all six models. P and L play important roles in reducing the concrete volume of spillway walls. Crest height is involved directly in the calculation of the three constraints (headwater ratio, relative thickness ratio, and cycle width ratio), and since the value of this constraint is within the acceptable range (according to Table 11), this height reduction does not result in loss of performance and safety of the spillway. The B parameter in the SFLA-RCP2.6 and IWO-RCP2.6 models is about 12 m less than the Ute spillway. The B parameter does not directly interfere in any constraint, but it is involved in calculating the wall length. In Figure 10, one cycle of all models is shown to compare B and W. The W_s in the Ute spillway was about 256 m, which was decreased to 223 m in the SFLA-RCP2.6 and IWO-RCP2.6 models. The W_s of each spillway is shown in Figure 11 for a better comparison.

Table 10 | Parameters of Ute and optimal models

		SFLA		IWO		CS	
Parameter	**Ute spillway**	**Base**	**RCP2.6**	**Base**	**RCP2.6**	**Base**	**RCP2.6**
Q (m^3/s)	16,143	16,145	12,250	16,144	12,251	16,144	12,250
N (–)	14.000	14.000	14.000	14.000	14.000	14.000	14.000
P (m)	9.140	8.022	7.963	8.050	7.967	8.395	8.063
T_w (m)	1.065	1.003	0.995	1.006	0.996	1.049	1.008
H_t (m)	5.790	6.511	6.202	6.513	6.201	6.751	6.279
B (m)	33.990	23.540	21.839	23.496	21.830	23.560	22.366
α (°)	12.162	17.836	17.500	17.812	17.500	17.761	17.500
A (m)	1.820	1.003	1.078	1.012	1.088	1.049	1.013
W (m)	18.290	17.154	15.927	17.121	15.943	17.192	16.130
W_s (m)	256.060	240.157	222.974	239.695	223.197	240.692	225.815
C_d (–)	0.383	0.457	0.400	0.457	0.400	0.432	0.385
L_s (m)	34.770	24.728	22.899	24.678	22.890	24.740	23.451
L_c (m)	73.181	51.462	47.953	51.380	47.956	51.578	48.928
L (m)	1,024.529	720.469	671.334	719.321	671.383	722.089	684.991
V_w (m^3)	9,972.916	5,795.709	5,321.531	5,826.764	5,328.667	6,360.948	5,566.052
V_e (m^3)	1,315.879	912.080	824.251	915.694	824.780	1,001.650	862.704
V_s (m^3)	3,500.596	2,634.222	2,290.550	2,626.148	2,292.138	2,676.167	2,365.893
V_T (m^3)	14,789.391	9,342.012	8,436.333	9,368.336	8,445.586	10,038.766	8,794.650

This parameter is important in locating spillways, especially in earth dams that their spillways are situated outside the main body of the dam. In fact, the limitation of this width is expressed as one of the main reasons for the choice of labyrinth spillways. The T_w is another parameter that contributes to the calculation of volume of spillway walls, which has decreased in the optimal models.

Increasing the angle of side legs (α) can increase the discharge coefficient. In optimal models, this parameter was increased by more than 30%. Totally, in the optimal models, the discharge coefficient, angle of side legs, and total head of the spillway were increased, and the height, thickness, length and width (spillway and apex) of the labyrinth spillway were decreased.

Table 11 | Results of models' constraints

		SFLA		IWO		CS	
Constraint	**Ute spillway**	**Base**	**RCP2.6**	**Base**	**RCP2.6**	**Base**	**RCP2.6**
$0.05 \leq H_t/P \leq 0.90$	0.634	0.812	0.779	0.809	0.778	0.804	0.779
$1.00 \leq A/T_w \leq 2.00$	1.709	1.000	1.083	1.005	1.093	1.000	1.005
$6.00 \leq P/T_w \leq 8.00$	8.582	8.000	8.000	7.999	7.998	7.999	7.999
$2.00 \leq W/P \leq 4.00$	2.001	2.138	2.000	2.127	2.001	2.048	2.001
$3.00 \leq L_c/W < 9.50$	4.001	3.000	3.011	3.001	3.008	3.000	3.033
$A/W \leq 0.0765$	0.099	0.059	0.068	0.059	0.068	0.061	0.063
$L_D/L_S \leq 0.35$	0.460	0.35	0.35	0.35	0.35	0.35	0.35

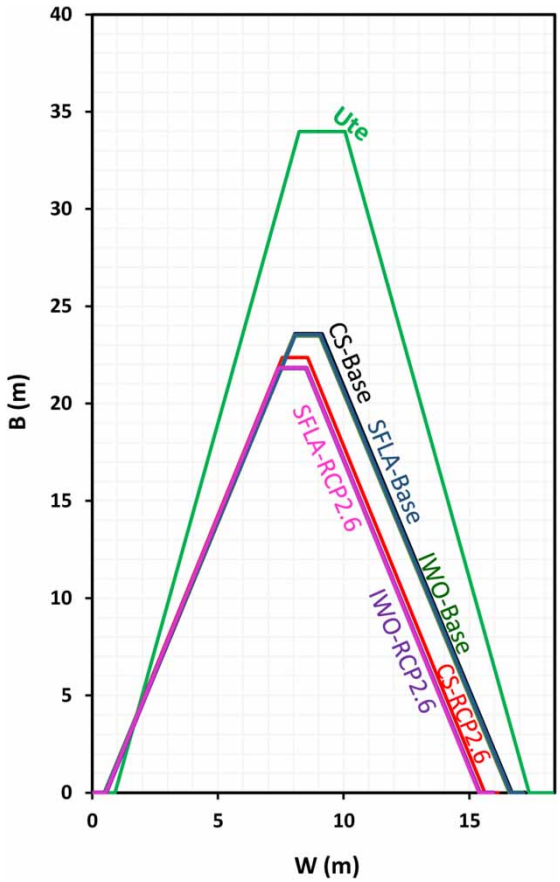

Figure 10 | One cycle of Ute and optimal labyrinth spillways.

As is obvious in Table 10, discharge constraint is more than the desired value. According to Table 11, other constraints in the design of Ute labyrinth spillway are in the desired range. In the Ute spillway, the value of the interference length ratio was 0.46, which was reduced to 0.35 in the optimal models. To increase the spillway capacity, the apex ratio (A/W) should be limited to $\leq$0.0765, which, according to Table 11, is not considered in the Ute design, but it is within the desired range in the proposed models.

CONCLUSION

In this paper, a novel approach was presented to investigate the effect of climate change uncertainty on the optimization of Ute Dam labyrinth spillway design. The concrete volume of the labyrinth spillway was selected as the objective function. The concrete volume may represent cost and environmental impacts of spillway construction. According to the present study results and historical streamflow data from 1941, the peak flow at the USGS 07226500 streamgage is decreasing. Hence, the design flood should be decreased. Results revealed that all three algorithms (SFLA, IWO, and CS) are able to optimize the problem. But, the SFLA was a little better in finding optimal solutions.

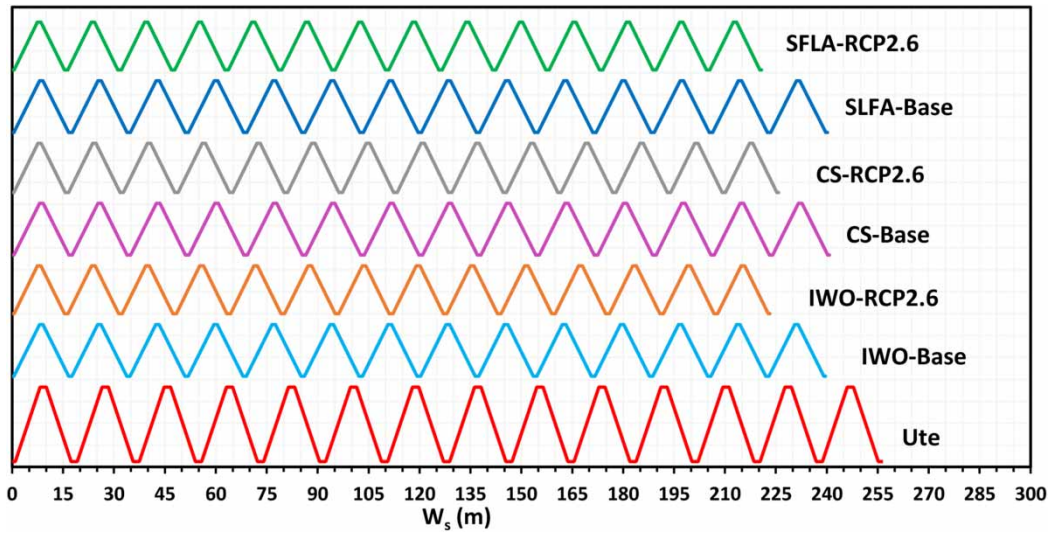

Figure 11 | Plan view of the Ute and optimal labyrinth spillways.

It is worth mentioning that because of different uncertainties that exist in methodology of this study such as the downscaling method and climate change scenarios, the present result is one of the possible solutions. For example, in the IHACRES model, the snow and vegetation cover were not considered, which might affect the streamflow and design flood. As was stated, IHACRES is a lumped model. In the future studies, other rainfall–runoff models (i.e., distributed or semi-distributed) can be used. In addition, in future studies, discharge volumes can be used in design flood estimation.

In brief, climate change, as a hydrologic uncertainty, has great impact on rainfall, temperature, streamflow, and design flood. Spillway geometry is strongly affected by design flood, and optimization algorithms can be very effective in reducing the spillway construction costs. By optimizing hydraulic structures geometry (e.g., reducing the concrete volume), such as spillways, construction time and other costs associated with extraction, production, transport, storage, destruction and recycling of materials may be reduced. These will also be effective in ameliorating environmental impacts.

CONFLICT OF INTEREST

We declare that we have no conflict of interest with any person or institution.

REFERENCES

Ashofteh, P. S., Bozorg-Haddad, O., Akbari-Alashti, H. & Marino, M. A. 2014 Determination of irrigation allocation policy under climate change by genetic programming. *Journal of Irrigation and Drainage Engineering* **141** (4), 04014059. doi:10.1061/(ASCE)IR.1943-4774.0000807.

Azimi, A. H. & Seyed Hakim, S. 2019 Hydraulics of flow over rectangular labyrinth weirs. *Irrigation Science* **37** (2), 183–193. doi:10.1007/s00271-018-0616-6.

Bates, B. C., Kundzewicz, Z. W., Wu, S. & Palutikof, J. P. (eds) 2008 *Climate Change and Water: Technical Paper of the Intergovernmental Panel on Climate Change*. IPCC Secretariat, Geneva, Switzerland.

Bhagat, N. 2017 Flood frequency analysis using Gumbel's distribution method: a case study of Lower Mahi Basin, India. *Journal of Water Resources and Ocean Science* **6** (4), 51–54. doi:10.11648/j.wros.20170604.11.

Bozorg-Haddad, O. (ed.) 2018 *Advanced Optimization by Nature-Inspired Algorithms*. Springer, Singapore. doi:10.1007/978-981-10-5221-7.

Bozorg-Haddad, O., Mirmomeni, M. & Mariño, M. A. 2010 Optimal design of stepped spillways using the HBMO algorithm. *Civil Engineering and Environmental Systems* **27** (1), 81–94. doi:10.1080/10286600802542465.

Brauer, D., Baumhardt, R. L., Gitz, D., Gowda, P. & Mahan, J. 2015 Characterization of trends in reservoir storage, streamflow, and precipitation in the Canadian River watershed in New Mexico and Texas. *Lake and Reservoir Management* **31** (1), 64–79. doi:10.1080/10402381.2015.1006348.

Chen, S. H. 2015 *Hydraulic Structures*. Springer. doi:10.1007/978-3-662-47331-3.

Croke, B. F. W., Andrews, F., Spate, J. & Cuddy, S. M. 2005 *IHACRES User Guide. Technical Report 2005/19*, 2nd edn. ICAM, School of Resources, Environment and Society, The Australian National University, Canberra.

Crookston, B. M. 2010 *Labyrinth Weirs*. PhD Dissertation, Utah State University, Logan, UT.

Crookston, B. M. & Tullis, B. P. 2012 Labyrinth weirs: nappe interference and local submergence. *Journal of Irrigation and Drainage Engineering* **138** (8), 757–765. doi:10.1061/(ASCE)IR.1943-4774.0000466.

Crookston, B. M. & Tullis, B. P. 2013 Hydraulic design and analysis of labyrinth weirs. I: discharge relationships. *Journal of Irrigation and Drainage Engineering* **139** (5), 363–370. doi:10.1061/(ASCE)IR.1943-4774.0000558.

Cunnane, C. 1989 *Statistical Distributions for Flood Frequency Analysis Operational*. Hydrology Report No. 33, World Meteorological Organization, No. 718, Geneva, Switzerland.

Dong, N. D., Jayakumar, K. V. & Agilan, V. 2018 Impact of climate change on flood frequency of the Trian Reservoir in Vietnam using RCMs. *Journal of Hydrologic Engineering* **23** (2), 05017032. doi:10.1061/(ASCE) HE.1943-5584.0001609.

Duricic, J., Erdik, T., Pektaş, A. O. & Van Gelder, P. H. A. J. M. 2013 Mean normalized force computation for different types of obstacles due to dam break using statistical techniques. *Water* **5** (2), 560–577. doi:10.3390/w5020560.

Ehteram, M., Mousavi, S. F., Karami, H., Farzin, S., Singh, V. P., Chau, K. W. & El-Shafie, A. 2018a Reservoir operation based on evolutionary algorithms and multi-criteria decision-making under climate change and uncertainty. *Journal of Hydroinformatics* **20** (2), 332–355. doi:10.2166/hydro.2018.094.

Ehteram, M., Singh, V. P., Karami, H., Hosseini, K., Dianatikhah, M., Hossain, M., Ming Fai, C. & El-Shafie, A. 2018b Irrigation management based on reservoir operation with an improved weed algorithm. *Water* **10** (9), 1267. doi:10.3390/w10091267.

Ehteram, M., Singh, V. P., Ferdowsi, A., Mousavi, S. F., Farzin, S., Karami, H., Mohd, N. S., Afan, H. A., Lai, S. H., Kisi, O., Malek, M. A., Ahmed, A. N. & El-Shafie, A. 2019 An improved model based on the support vector machine and cuckoo algorithm for simulating reference evapotranspiration. *PLoS One* **14** (5), e0217499. doi: 10.1371/journal.pone.0217499.

Erdik, T. 2009 Fuzzy logic approach to conventional rubble mound structures design. *Expert Systems with Applications* **36** (3), 4162–4170. doi:10.1016/j.eswa.2008.06.012.

Erdik, T. & Savci, M. E. 2008 TAKAGI-SUGENO fuzzy approach in rock armored slopes for 2% wave runup estimation. *Coastal Engineering Journal* **50** (2), 161–177. doi:10.1142/S0578563408001776.

Erdik, T., Savci, M. E. & Şen, Z. 2009 Artificial neural networks for predicting maximum wave runup on rubble mound structures. *Expert Systems with Applications* **36** (3), 6403–6408. doi:10.1016/j.eswa.2008.07.049.

Erdik, T., Duricic, J. & Van Gelder, P. H. A. J. M. 2013 The probabilistic assessment of overtopping reliability on Akyayik dam. *KSCE Journal of Civil Engineering* **17** (7), 1810–1819. doi:10.1007/s12205-013-1355-0.

Eusuff, M. M. & Lansey, K. E. 2003 Optimization of water distribution network design using the shuffled frog leaping algorithm. *Journal of Water Resources Planning and Management* **129** (3), 210–225. doi:10.1061/(ASCE)0733-9496(2003)129:3(21 0).

Falvey, H. T. 2003 *Hydraulic Design of Labyrinth Weirs*. ASCE Press, Reston, VA. doi:10.1061/9780784406311.

Ferdowsi, A., Farzin, S., Mousavi, S. F. & Karami, H. 2019 Hybrid bat and particle swarm algorithm for optimization of labyrinth spillway based on half and quarter round crest shapes. *Flow Measurement and Instrumentation* **66**, 209–217. doi:10.1016/j.flowmeasinst.2019.03.003.

Fill, H. D. & Steiner, A. A. 2003 Estimating IPF from mean daily flow data. *Journal of Hydrologic Engineering* **8** (6), 365–369. doi:10.1061/(ASCE)1084-0699(2003)8:6(365).

Fuller, W. E. 1914 Flood flows. *Transations of the ASCE* **77**, 564–617.

Ghaderi, A., Abbasi, S., Abraham, J. & Azamathulla, H. M. 2020 Efficiency of trapezoidal labyrinth shaped stepped spillways. *Flow Measurement and Instrumentation* **72**, 101711. doi:10.1016/j.flowmeasinst.2020.101711.

Ghare, A. D., Mhaisalkar, V. A. & Porey, P. D. 2008 An approach to optimal design of trapezoidal labyrinth weirs. *World Applied Sciences Journal* **3** (6), 934–938.

Guo, S., Muhammad, R., Liu, Z., Xiong, F. & Yin, J. 2018 Design flood estimation methods for cascade reservoirs based on copulas. *Water* **10** (5), 560. doi:10.3390/w 10050560.

Haan, C. T. 1977 *Statistical Methods in Hydrology*. Iowa State University Press, Ames, IA.

Hager, W. H., Pfister, M. & Tullis, B. P. 2015 Labyrinth weirs: developments until 1985. In *E-Proceedings of the 36th IAHR World Congress*, June 28–July 3, Hague, Netherlands.

Hassanvand, M. R., Karami, H. & Mousavi, S. F. 2019 Use of multi-criteria decision-making for selecting spillway type and optimizing dimensions by applying the harmony search algorithm: Qeshlagh dam case study. *Lakes & Reservoirs: Research and Management* **24** (1), 66–75. doi:10.1111/lre.12250.

Hepler, T. 1992 Innovative spillway designs. In *Proceedings of the Hydraulic Engineering Sessions at Water Forum 92, Hydraulic Engineering: Saving A Threatened Resource-In Search of Solutions*, August 2–6, Baltimore, Maryland.

Hosseini, K., Nodoushan, E. J., Barati, R. & Shahheydari, H. 2016 Optimal design of labyrinth spillways using meta-heuristic algorithms. *KSCE Journal of Civil Engineering* **20** (1), 468–477. doi:10.1007/s12205-015-0462-5.

Houston, K. L. 1982 *Hydraulic Model Study of Ute Dam Labyrinth Spillway*. Report GR-82-7.

Indelkofer, H. & Rouve, G. 1975 Discharge over polygonal weirs. *Journal of the Hydraulics Division* **110** (HY3), 385–401.

Jakeman, A. J., Littlewood, I. G. & Whitehead, P. G. 1990 Computation of the instantaneous unit hydrograph and identifiable component flows with application to two small upland catchments. *Journal of Hydrology* **117** (1–4), 275–300. doi:10.1016/0022-1694(90)90097-H.

Karamouz, M., Doroudi, S., Ahmadi, A. & Moridi, A. 2009 Optimal design of water diversion system: a case study. In: *World Environmental and Water Resources Congress 2009: Great Rivers 1–10*. doi:10.1061/41036(342)342.

Karamouz, M., Nazif, S. & Zahmatkesh, Z. 2013 Self-organizing Gaussian-based downscaling of climate data for simulation of urban drainage systems. *Journal of Irrigation and Drainage Engineering* **139** (2), 98–112. doi:10.1061/(ASCE) IR.1943-4774.0000500.

Kardan, N., Hassanzadeh, Y. & Bonab, B. S. 2017 Shape optimization of trapezoidal labyrinth weirs using genetic algorithm. *Arabian Journal for Science and Engineering* **42** (3), 1219–1229. doi:10.1007/s13369-016-2355-4.

Kaveh, A. 2017 *Advances in Metaheuristic Algorithms for Optimal Design of Structures*, 2nd edn. Springer, Switzerland. doi:10.1007/978-3-319-05549-7.

Khatsuria, R. M. 2004 *Hydraulics of Spillways and Energy Dissipators*. CRC Press, New York.

Khode, B. V. & Tembhurkar, A. R. 2010 Evaluation and analysis of crest coefficient for labyrinth weir. *World Applied Sciences Journal* **11** (7), 835–839.

King, J. P., Hawley, J. W., Hernandez, J., Kennedy, J. F. & Martinez, E. L. 2006 *Study of Potential Water Salvage on the Tucumcari Project Arch Hurley Conservancy District*. New Mexico Water Resources Institute, New Mexico State University, Report TR335.

Li, Y., Zhou, J., Zhang, Y., Qin, H. & Liu, L. 2010 Novel multiobjective shuffled frog leaping algorithm with application to reservoir flood control operation. *Journal of Water Resources Planning and Management* **136** (2), 217–226. doi:10.1061/_ASCE_ WR.1943-5452.0000027.

Mirnaseri, M. & Emadi, A. 2014 Hydraulic performance of combined flow labyrinth weir-gate. *Advance in Agriculture and Biology* **2**, 54–60. doi:10.15192/PSCP.AAB.2014.1.2.5460.

Monsef, H., Naghashzadegan, M., Jamali, A. & Farmani, R. 2019 Comparison of evolutionary multi objective optimization algorithms in optimum design of water distribution network. *Ain Shams Engineering Journal* **10** (1), 103–111. doi:10.1016/j.asej.2018.04.003.

Moriasi, D. N., Arnold, J. G., Van Liew, M. W., Bingner, R. L., Harmel, R. D. & Veith, T. L. 2007 Model evaluation guidelines for systematic quantification of accuracy in watershed simulations. *Transactions of the ASABE* **50** (3), 885–900.

Najafi, M. R., Moradkhani, H. & Jung, I. W. 2011 Assessing the uncertainties of hydrologic model selection in climate change impact studies. *Hydrological Processes* **25** (18), 2814–2826. doi:10.1002/hyp.8043.

Nazif, S. & Karamouz, M. 2014 Evaluation of climate change impacts on streamflow to a multiple reservoir system using a data-based mechanistic model. *Journal of Water and Climate Change* **5** (4), 610–624. doi:10.2166/wcc.2014.012.

Novak, P., Moffat, A. I. B., Nalluri, C. & Narayanan, R. 2014 *Hydraulic Structures*. CRC Press, New York.

Onen, F. & Bagatur, T. 2017 Prediction of flood frequency factor for Gumbel distribution using regression and GEP model. *Arabian Journal for Science and Engineering* **42** (9), 3895–3906. doi:10.1007/s13369-017-2507-1.

Orouji, H., Bozorg Haddad, O., Fallah-Mehdipour, E. & Marino, M. A. 2012 Estimation of Muskingum parameter by meta-heuristic algorithms. *Proceedings of the Institution of Civil Engineers-Water Management* **165** (6), 1–10.

Orouji, H., Mahmoudi, N., Fallah-Mehdipour, E., Pazoki, M. & Biswas, A. 2016 Shuffled frog-leaping algorithm for optimal design of open channels. *Journal of Irrigation and Drainage Engineering* **142** (10), 06016008. doi:10.1061/(ASCE)IR.1943-4774.0001059.

Pektas, A. O. & Erdik, T. 2014 Peak discharge prediction due to embankment dam break by using sensitivity analysis based ANN. *KSCE Journal of Civil Engineering* **18** (6), 1868–1876. doi:10.1007/s12205-014-0047-8.

Raju, K. S. & Kumar, D. N. 2018 *Impact of Climate Change on Water Resources with Modeling Techniques and Case Studies*. Springer, Singapore. doi:10.1007/978-981-10-6110-3.

Safarrazavi Zadeh, M., Esmaeili Varaki, M. & Biabani, R. 2019 Experimental study on flow over sinusoidal and semicircular labyrinth weirs. *ISH Journal of Hydraulic Engineering* 1–10. doi:10.1080/09715010.2019.1644679.

Safavi, H. R., Sajjadi, S. M. & Raghibi, V. 2017 Assessment of climate change impacts on climate variables using probabilistic ensemble modeling and trend analysis. *Theoretical and Applied Climatology* **130** (1–2), 635–653. doi:10.1007/s00704-016-18983.

Sangal, B. P. 1983 Practical method of estimating peak flow. *Journal of Hydraulic Engineering* **109** (4), 549–563. doi:10.1061/(ASCE)0733-9429(1983)109:4(549).

Sangsefidi, Y., Mehraein, M., Ghodsian, M. & Motalebizadeh, M. R. 2017 Evaluation and analysis of flow over arced weirs using traditional and response surface methodologies. *Journal of Hydraulic Engineering* **143** (11), 04017048. doi:10.1061/(ASCE)HY.1943-7900.0001377.

Sarzaeim, P., Bozorg-Haddad, O., Fallah-Mehdipour, E. & Loáiciga, H. A. 2017 Environmental water demand assessment under climate change conditions. *Environmental Monitoring and Assessment* **189** (7), 359. doi:10.1007/s10661-017-6067-3.

Sarzaeim, P., Bozorg-Haddad, O., Zolghadr-Asli, B., Fallah-Mehdipour, E. & Loáiciga, H. A. 2018 Optimization of run-of-river hydropower plant design under climate change conditions. *Water Resources Management* **32** (12), 3919–3934. doi:10.1007/s11269-018-2027-0.

Spencer, S. & Salazar, A. 2010 *Historical Trends in key Components of the Hydrologic Cycle for the Lake Meredith Watershed*. Available from: http://www.panhandlewater.org/2011 adopted plan.html.

Tabari, M. M. R. & Hashempour, M. 2019 Development of GWO–DSO and PSO–DSO hybrid models to redesign the optimal dimensions of labyrinth spillway. *Soft Computing* **23**, 6391–6406. doi:10.1007/s00500-018-3292-9.

Taguas, E. V., Ayuso, J. L., Pena, A., Yuan, Y., Sanchez, M. C., Giraldez, J. V. & Pérez, R. 2008 Testing the relationship between instantaneous peak flow and mean daily flow in a Mediterranean Area Southeast Spain. *Catena* **75** (2), 129–137. doi:10.1016/j .catena.2008.04.015.

Tullis, J. P., Amanian, N. & Waldron, D. 1995 Design of labyrinth spillways. *Journal of Hydraulic Engineering* **121** (3), 247–255. doi:10.1061/(ASCE)0733-9429 (1995)121:3(247).

Wilby, R. L., Dawson, C. W. & Barrow, E. M. 2002 SDSM – a decision support tool for the assessment of regional climate change impacts. *Environmental Modelling & Software* **17** (2), 145–157. doi:10.1016/S1364-8152(01)00060-3.

Wilks, D. S. 1993 Comparison of three-parameter probability distributions for representing annual extreme and partial duration precipitation series. *Water Resources Research* **29** (10), 3543–3549. doi:10.1029/93WR01710.

Willmore, C. 2004 *Hydraulic Characteristics of Labyrinth Weirs*. MSc Thesis, Utah State University, Logan, UT.

Wilson, L. & O'Brien, V. 2000 *Canadian River Watershed: Brush Control Planning, Assessment and Feasibility Study*. Available from: http://www.tsswcb.texas.gov/reports#feasibilitystudy.

Xing, W., Wang, W., Shao, Q. & Ding, Y. 2018 Estimating net irrigation requirements of winter wheat across central-eastern China under present and future climate scenarios. *Journal of Irrigation and Drainage Engineering* **144** (7), 05018005. doi:10.1061/(ASCE)IR.1943-4774.0001320.

Yang, X. S. 2010 *Nature-Inspired Metaheuristic Algorithms*, 2nd edn. Luniver Press, Frome, UK.

Yang, X. S. (ed.) 2018 *Nature-inspired Algorithms and Applied Optimization*. Springer. doi:10.1007/978-3-319-67669-2.

Zahmatkesh, Z., Karamouz, M., Goharian, E. & Burian, S. J. 2015 Analysis of the effects of climate change on urban storm water runoff using statistically downscaled precipitation data and a change factor approach. *Journal of Hydrologic Engineering* **20** (7), 05014022. doi:10.1061/(ASCE)HE.1943-5584.0001064.

First received 24 January 2020; accepted in revised form 22 April 2020. Available online 5 June 2020